PHYSICAL REVIEW B VOLUME 18, NUMBER 10 15 NOVEMBER, 1978

Self-consistent electronic structure of transition-metal surfaces: The Mo (001) surface

G. P. Kerker,* K. M. Ho, and Marvin L. Cohen
Department of Physics, University of California and Materials and Molecular Research Division, Lawrence Berkeley Laboratory, Berkeley, California 94720
(Received 5 June 1978)

A self-consistent pseudopotential method together with a mixed-basis set of plane waves and Gaussian orbitals are used to determine the electronic structure of the (001) surface of molybdenum. The pseudopotential is derived from a self-consistent calculation of the atomic levels and wave functions, and is tested for bulk molybdenum. The resulting bulk band structure and density of states are compared with existing augmented plane-wave calculations. The same potential is applied to investigate the electronic structure of an uncontracted Mo (001) surface. A complete analysis of the surface states is given in terms of their distribution in the two-dimensional surface Brillouin zone, charge-density distribution, and the local density of states. The results are in very good agreement with recent photoemission measurements.

I. INTRODUCTION

Clean and adsorbate-covered transition-metal surfaces have attracted increasing interest within the last few years because of refined experimental techniques that are now available to probe these surfaces. Angle-resolved photoemission, ion-neutralization, and Auger-electron spectroscopy, as well as field emission and low-energy electron diffraction (LEED), are some of the tools that have been used to obtain information about the geometry and the electronic structure of clean surfaces and surfaces covered with foreign atoms.

Despite the growing amount of experimental data and of the importance of transition-metal surfaces as possible catalysts, the theoretical determination of the electronic structure of these surfaces still poses problems due to the presence and the localized nature of the valence d electrons. Many theoretical approaches have been used to calculate the electronic properties of transition-metal surfaces, most of them based on a tight-binding picture of the d electrons. A summary of the various methods is presented in Ref. 1.

The aim of this paper is to give a complete and self-consistent description of the (001) surface of molybdenum. Although the surface properties of tungsten have probably been studied most extensively, this material is expected to show important relativistic effects. At present we have not yet incorporated relativistic effects into our method, and we have therefore chosen molybdenum assuming that relativistic effects are far less important in this material. In fact, our results for the surface electronic structure of Mo support this assumption, since spin-orbit interactions are not necessary to explain the existence of any of the experimentally observed surface states.

Recent angle-resolved photoemission experiments applied to a clean Mo (001) surface reveal two sharp peaks at 0.3 and 3.3 eV below the Fermi level E_F at normal emission, which are very sensitive to surface contamination.[2-5] They are also observed for nonvanishing emission angles, together with a third peak that appears about 0.6 eV below E_F.[4,5] It should be noticed that these peak structures also occur in tungsten at slightly lower energies compared to the Fermi level.[5]

The theoretical approaches made so far to explain the surface structure of Mo(001) and also Mo(011) have some rather incomplete features. Noguera *et al.*[4,6] calculated the density of states for both surfaces using a Korringa-Kohn-Rostoker method, which builds up the semi-infinite crystal from a sequence of layers. A non-self-consistent sharp potential step at the surface was used to separate the vacuum from the solid. A surface state that could account for the peak structure at normal emission near E_F was found only after relaxing the sharp potential barrier and including a 13% contraction of the first interlayer spacing in the case of Mo(001). The actual size of the contraction, which was deduced from LEED experiments,[7] is, however, controversial, and is believed to be much smaller.[8]

Weng,[9] using a tight-binding Green's-function method, was able to predict surface resonances away from normal emission in satisfactory agreement with the experimental results; however, this approach did not explain the existence of a strong surface resonance or surface state at E_F at normal emission. All the above calculations were done without screening the ionic potentials at the surface self-consistently. From the similarity of the total surface charge density with the corresponding bulk charge density of transition metals, it was argued[6] that self-consistency is less important than in semiconductors. We have, however, found considerable differences in the screened potential at the surface as compared to the screened

bulk potential in Mo, which makes the use of bulk-type potentials for the surface atoms, as was done in Refs. 4 and 6, almost prohibitive.

We present in this paper the first self-consistent calculation of the electronic structure of an Mo (001) surface using a pseudopotential method. The analysis of our results, which have been briefly reported recently,[10] includes not only the surface density of states, but also the individual surface resonance bands, their charge-density distribution in real space, and their k-space behavior. We did not assume the tight-binding approximation, and treated the s, p, and d electrons on an equal footing.

The method consists essentially of solving the Schrödinger equation in the local-density formalism. This method is used to get a nonlocal pseudopotential that describes the ion cores in the ground-state configuration of the atom from a self-consistent calculation of the atomic levels and wave functions. Adopting the frozen core approximation, this potential is used to obtain the bulk and surface electronic properties. A slab superlattice is used for the surface calculation to achieve periodicity perpendicular to the surface. In order to account both for the highly localized valence d electrons and the delocalized s- or p-like electrons, the wave function for the crystal is expanded in a formally overcomplete set of plane waves and Bloch functions made of localized orbitals.

The details of the calculational techniques are described in Sec. II. The results for the bulk and surface and the comparison with experiment are presented in Sec. III. The paper is concluded with a summary in Sec. IV.

II. CALCULATIONAL TECHNIQUES

The electronic band structure of both the bulk and the (001) surface of Mo is calculated from a one-particle pseudopotential Hamiltonian

$$H = p^2/2m + V_{\rm ps} + V_{\rm COUL} + V_x \,. \tag{1}$$

$V_{\rm COUL}$ is the usual electronic Coulomb potential that is obtained from the total pseudo charge density $\rho(\vec{r})$ by using Poisson's equation

$$V_{\rm COUL}(\vec{r}) = e^2 \int \frac{\rho(\vec{r}')}{|\vec{r} - \vec{r}'|} d^3r' \,. \tag{2}$$

V_x is an exchange potential, which is given in the local density formalism to lowest order by the well-known "$\rho^{1/3}$" term[11,12]

$$V_x(\vec{r}) = -\tfrac{3}{2}\alpha e^2 (3/\pi)^{1/3} \rho^{1/3}(\vec{r}) \,. \tag{3}$$

The choice of the exchange parameter α is not very crucial to the final results as long as its value lies between $\frac{2}{3}$ and 1. In accordance with Ref. 1 we have chosen α to be 0.80 in this work. The sum of $V_{\rm COUL}$ and V_x acts as a potential that screens the effect of the ionic cores. The ions are described by a superposition of nonlocal Mo^{6+} ionic pseudopotentials

$$V_{\rm ps}(\vec{r}, \vec{r}') = \sum_{\vec{R}_n} v_{\rm ps}(\vec{r} - \vec{R}_n, \vec{r}' - \vec{R}_n) \,, \tag{4}$$

where the sum is over all atomic positions and $v_{\rm ps}$ is a nonlocal atomic pseudopotential. V is used to denote crystal potentials and v is used for atomic potentials. Since the different angular components of the wave function see a different core repulsion due to core orthogonalization, we write

$$v_{\rm ps} = \sum_l v_l P_l \,, \tag{5}$$

where the operator P_l projects out the lth angular momentum component of the wave function. Using the completeness relation

$$\sum_l P_l = 1 \,, \tag{6}$$

Eq. (5) can be rewritten as a sum of a local potential $v_{\rm L}$ that acts on all angular components of the wave function in the same way and a nonlocal correction $\Delta v_{\rm NL}$ that acts on the various l components differently:

$$v_{\rm ps} = v_{\rm L} + \Delta v_{\rm NL} = v_{\rm L} + \sum_l (v_l - v_{\rm L}) P_l \,. \tag{7}$$

Notice that $v_{\rm ps}$ is a nonlocal operator because of the presence of the projection operator. In real-space coordinates, Eq. (7) reads

$$v_{\rm ps}(\vec{r}, \vec{r}') = \delta(\vec{r} - \vec{r}')\, v_{\rm L}(r) + \delta(r - r') \times \frac{1}{r^2} \sum_l [v_l(r) - v_{\rm L}(r)] P_l(\theta, \varphi; \theta', \varphi') \,, \tag{8}$$

where $\vec{r} = (r, \theta, \varphi)$, $\vec{r}' = (r', \theta', \varphi')$, and

$$P_l(\theta, \varphi; \theta', \varphi') = \sum_m Y_{lm}(\theta, \varphi)\, Y_{lm}^*(\theta', \varphi') \,. \tag{9}$$

Y_{lm} is the usual spherical harmonic with angular-momentum quantum numbers l and m. We use the s component of the expansion Eq. (5) as a local potential $v_{\rm L}$, and keep a p and a d nonlocal correction.

The potentials $v_s(r)$, $v_p(r)$, and $v_d(r)$ are obtained as follows. The core part of the self-consistent $X\alpha$ atomic potential for the ground state of Mo computed with Herman and Skillman's atomic-structure program[13] is removed to obtain smooth and nodeless $4d$, $5s$, and $5p$ wave functions with the same energy as the all-electron result. Fur-

thermore, we require that the pseudo wave function matches the $X\alpha$ wave function outside the core region. In practice, this means that the pseudopotential starts deviating from the $X\alpha$ result between the outermost maximum and the outermost node of the radial $X\alpha$ wave function. The shape of the pseudopotential in the core region is relatively insensitive to the band structure when it is used in bulk or surface calculations. Since we mainly work in Fourier space, where smooth nonsingular potentials can be conveniently treated, we chose a parabola to simulate the repulsion in the core region. The result of this calculation is shown in Fig. 1(a) together with the $4d$, $5s$, and $5p$ atomic pseudo wave functions. The unscreened core

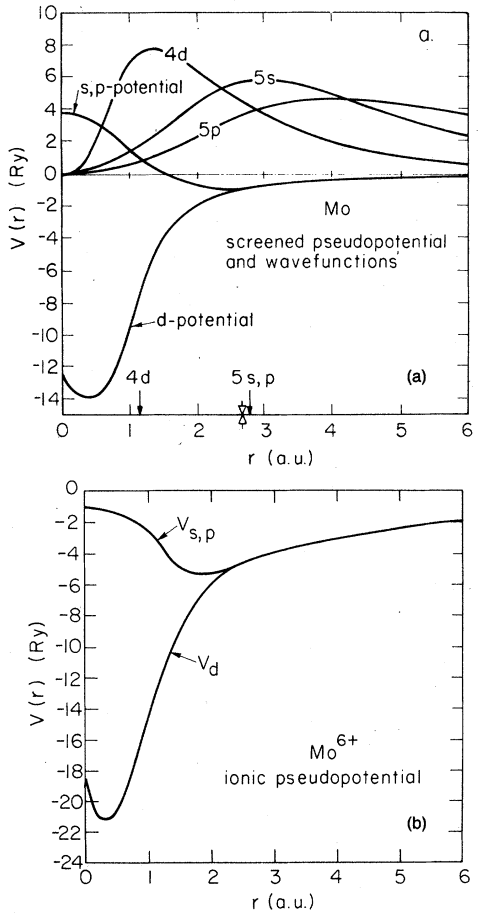

FIG. 1. (a) Self-consistently-screened pseudopotential for the Mo atom decomposed in its angular-momentum components as a function of r. Also plotted are the pseudo radial eigenfunctions $rR_{nl}(r)$ for the valence states. Inside the core potentials, the wave functions deviate from the all-electron result. The core region is normally different for different angular momenta l. The core radius is marked by an arrow for the various l values. The double arrow indicates half the nearest-neighbor distance in the metal. (b) Mo^{+6} ionic pseudopotentials. v_s, v_p, and v_d are plotted as functions of r.

potentials V_s, V_p, and V_d are obtained by subtracting the (pseudo)atomic screening potential $v_H + v_x$ (the Hartree and exchange potentials) from the screened pseudopotentials. The quality of the core potentials is checked by calculating the energies and wave functions of the neutral Mo atom in various *excited* configurations, and comparing the results with $X\alpha$-type calculations. A plot of the core potentials is given in Fig. 1(b). As in the case of Nb, the d electrons see a much stronger potential than the s and p electrons. The s and p core potentials are practically identical.

To solve the Schrödinger equation self-consistently for the Hamiltonian [Eq. (1)], we use an iterative procedure that is started by approximating $V_{ps} + V_{coul} + V_x$ by a pseudopotential constructed from a superposition of the atomic core pseudopotentials obtained above. From the valence charge density, a new screening potential is obtained and put back into the Hamiltonian. The procedure is repeated until the input and output screening potentials agree with each other within 0.01 Ry.

To account for the highly localized d part of the total wave function, as well as for the delocalized s and p contributions, it is very convenient to expand the crystal wave function in a mixed set of plane waves and Bloch functions made of localized orbitals[14]:

$$\psi_n(\vec{k},\vec{r}) = \sum_{\vec{G}} a_n(\vec{k}+\vec{G})\, e^{i(\vec{k}+\vec{G})\cdot\vec{r}} + \sum_{\lambda} b^n_{j,\lambda}(\vec{k})\, \phi_{j\lambda}(\vec{k},\vec{r})\,. \tag{10}$$

$\vec{k}$ is a Bloch wave vector, n is the band index, and $\vec{G}$ denotes a reciprocal-lattice vector. The subscript j counts the number of atoms per unit cell (for simplicity the formalism is presented for only one type of atoms per unit cell). The subscript λ is an abbreviation for the angular-momentum quantum numbers l and m. The basis functions $\phi_{j\lambda}$ are Bloch functions constructed from localized orbital functions $d_\lambda(\vec{r})$:

$$\phi_{j\lambda}(\vec{k},\vec{r}) = \sum_{\mu\nu} e^{i\vec{k}\cdot(\vec{R}_\mu+\vec{\tau}_\nu)} d_\lambda(\vec{r}-\vec{R}_\mu-\tau_\nu)\,\theta_{j\nu}\,. \tag{11}$$

The sum is over all lattice sites $\vec{R}_\mu$ and atomic positions $\vec{\tau}_\nu$ in a unit cell. The coefficients $\theta_{j\nu}$ are determined such that only real matrix elements occur in the diagonalization procedure. This can always be achieved if the lattice has inversion symmetry as in the case of bcc Mo.

We choose $d_\lambda(\vec{r})$ to be a linear combination of Gaussian orbitals

$$d_\lambda(\vec{r}) \equiv N_{lm} r^l K_{lm}(\theta,\varphi) \sum_i C_{lm,i}\, e^{-\gamma_i r^2}\,. \tag{12}$$

N_{lm} is a normalization constant and K_{lm} is a cubic harmonic[15] of angular-momentum quantum number l. For $l=2$ the subscript m runs from 1 to 5, but it is actually no longer associated with the z-component quantum number of the angular momentum, because the cubic harmonics are linear combinations of spherical harmonics. The coefficients $C_{lm,i}$ and the exponents γ_i are determined by fitting the localized orbital $d_\lambda(\vec{r})$ to the atomic d pseudo wave function. It turns out that for Mo it is sufficient to use only one Gaussian orbital with $C_{lm}=1.0$ and $\gamma=0.80$. This choice of the parameters places the maximum of the radial part of $d_\lambda(\vec{r})$ at the position of the maximum of the radial atomic pseudo wave function. However, the decay length of the orbital $d_\lambda(\vec{r})$ is much shorter than the decay length of the atomic wave function. If one assumes that the d part of the crystal wave function is very similar to the atomic d wave function, the basis functions $\phi_{j,\lambda}(\vec{k},\vec{r})$ are certainly not sufficient to represent the d character of the crystal wave function properly; however, the error is compensated by including an appropriate amount of plane waves in the expansion [Eq. (10)]. This flexibility makes a mixed-basis expansion an extremely practical scheme to deal with for transition metals.

From the expansion [Eq. (10)] we obtain the eigenvalue problem

$$\sum_{\alpha'}(H_{\alpha\alpha'}-ES_{\alpha\alpha'})C_{\alpha'}=0\,, \tag{13}$$

where the indices α, α' stand for the plane waves $|\vec{k}+\vec{G}\rangle$ and the Bloch functions $|\phi_{j\lambda}(\vec{k})\rangle$. The coefficients C_α represent the coefficients $a_n(\vec{k}+\vec{G})$ or $b^n_{j\lambda}(\vec{k})$ of expansion (10), depending on the index α. $S_{\alpha\alpha'}$ is the usual overlap matrix element. The matrix eigenvalue problem is solved by using the Choleski decomposition of S.[16]

Although expansion (10) is formally overcomplete, overcompleteness is not reached if we include a finite number of plane waves in the expansion. Numerical instabilities that occur if one approaches overcompleteness can be avoided by monitoring the eigenvalues of the overlap matrix, which should be of the order of 1.[17] Some details of the evaluation of the various matrix elements within the mixed-basis scheme are given in Appendix A.

The method applies equally well to calculate the electronic properties of the bulk material and the surface, provided one is able to regain periodicity perpendicular to the surface. This is achieved by employing the slab method,[18] which has now become standard technique for treating surfaces. The surface of the semi-infinite crystal is simulated by either of the two noninteracting surfaces of a thin slab that are exposed to a finite number of empty-space layers. This arrangement is repeated throughout all space. In the case of Mo we have found that a five-layer Mo (001) slab exposed to three-layer vacuum on each side gives a good description of the electronic structure of this surface.

III. RESULTS

A. Bulk molydenum

In order to test the quality of our pseudopotentials and to obtain a projected band structure for the surface calculation, we calculated the band structure and the density of states of the bulk material. The advantage of using a mixed-basis set to expand the wave function manifests itself in the number of basis functions that have to be included in the expansion in order to get stable eigenvalues. Whereas a pure plane-wave expansion requires the diagonalization of an 80×80 matrix, only about 50 basis functions, that is, 45 plane waves and five d-type orbitals, were necessary within the mixed-basis scheme to get the energy levels stable within 0.2 eV. Both methods converge to the same results at self-consistency.[19]

To get the self-consistent potential, we used eight special $\vec{k}$ points[20] in the $\frac{1}{48}$ irreducible part of the Brillouin zone (BZ). The Fermi level E_F is determined by

$$2\sum_{\vec{k}_i=1}^{8}\sum_n w(\vec{k}_i)\,\Theta(E_F-E_n(\vec{k}_i))=z\,, \tag{14}$$

where z is the number of electrons per primitive unit cell, six in the case of bulk Mo. Θ is the step function and $w(\vec{k}_i)$ is a weight factor that measures the weight of the vector k_i according to its volume in the BZ. The total valence charge density is then given by

$$\rho(\vec{r})=\sum_{\vec{k}\in BZ}\sum_{\substack{\vec{k},n\\ E_n(\vec{k})\le E_F}}|\psi_n(\vec{k},\vec{r})|^2\,. \tag{15}$$

With the self-consistent screening potential obtained from the total charge density $\rho(\vec{r})$, the energy eigenvalues along various high-symmetry lines in the BZ are calculated. The results are displayed in Fig. 2. The separation between energy levels tends to be smaller than in non-self-consistent augmented-plane-wave (APW) calculations, e.g., $E_F-E(\Gamma_1)=5.6$ eV and $E(H_{25'})-E(H_{12})=8.37$ eV in the present calculation, whereas APW calculations[21] give 6.64 and 9.36 eV, respectively. We believe this to be a result of self-consistency, since our starting potential, which is a superposition of atomically screened core potentials, gives almost perfect agreement for the energy levels with non-self-consistent APW results. One

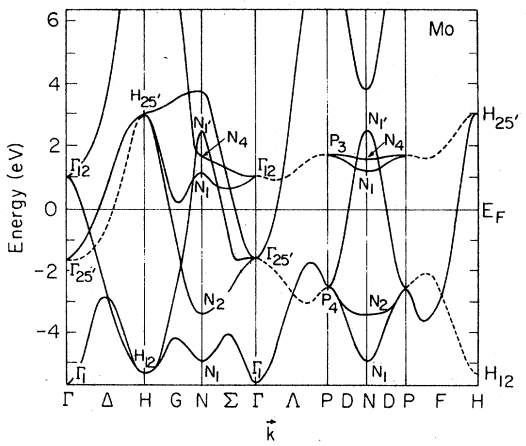

FIG. 2. Energy bands along symmetry directions for bulk Mo. Dashed lines are doubly degenerate levels.

major discrepancy occurs at the N symmetry point where the unoccupied $E(N_{1'})$ level may be somewhat high in energy. The results of the only self-consistent APW calculation on Mo by Moruzzi *et al.*,[22] which have not yet been published, indicate that this level might fall in between the levels $E(N_1)$ and $E(N_4)$, thus closing the gap that exists in Nb between $E(N_{1'})$ and $E(N_1)$. This has important consequences for the projection of the bulk band structure onto the (001) surface BZ, and hence for the occurrence of surface states in the corresponding region of the surface BZ, as we shall see later. A comparison of the energy levels at some symmetry points in the bulk BZ is given in Table I for (i) the non-self-consistent, non-relativistic APW calculation by Petroff and Viswanathan[2]; (ii) a corresponding self-consistent calculation by Moruzzi *et al.*[21] (as far as the unpublished data were available); and (iii) for the present calculation. Also given is the bulk density of states, which is obtained from 35 selected $\vec{k}$ points in the irreducible part of the BZ by a fast Fourier-series-expansion technique[23] (Fig. 3). Although we were not primarily interested in getting a highly resolved density of states, the principal peaks agree reasonably well with photoemission data and APW results (Table II).

B. (001) surface

The electronic structure of the (001) surface is obtained by applying the same method to the above described "slab-crystal." Here, the advantage of using a mixed-basis set to expand the wave function becomes even more obvious. Whereas the calculation of the Nb (001) surface properties required ~110 plane waves per atom, we were able to cut back the number of basis function to ~45 per atom by including one Gaussian orbital per atom in the slab unit cell. Convergence tests showed that the most sensitive d levels were stable within 0.2 eV when the number of basis functions were increased.

The (001) face of the bcc lattice is a square with length a_c, which is the bcc cubic lattice constant. The corresponding two-dimensional BZ is shown in Fig. 4. The symmetry lines $\bar{\Delta}$, $\bar{Y}$, and $\bar{\Sigma}$ enclose the irreducible part (1/8th) of the surface BZ. The screening potential during iteration is obtained from the charge density based on three special $\vec{k}$ points[24]; however, for the final potential, a regular mesh of 15 $\vec{k}$ points in the irreducible part of the surface BZ is used.

The local part of the screened total self-consistent potential, that is, core plus screening potential, is plotted along the z axis perpendicular to the surface (Fig. 5). The slab is approached from the left- to the right-hand side. From the Fermi energy E_F, which is represented by a straight line, one can deduce a work function value of 4.3 eV. The experimentally measured value for the Mo (001) surface is 4.58 eV.[6] It can also be seen from this figure that the screening around the surface atoms differs from the screening in the slab interior. In particular, the potential above the surface layer is much less attractive due to the

TABLE I. Comparison of the bulk energy levels at some symmetry points with other band-structure calculations. The levels are quoted with respect to $E(\Gamma_1)$.

	APW non-self-consistent (Ref. 21)	APW self-consistent (Ref. 22)	Pseudopotential (present work)
Γ_1	0	0	0
$\Gamma_{25'}$	5.55	5.09	3.97
Γ_{12}	8.11	7.85	6.59
H_{12}	1.16	0.57	0.27
$H_{25'}$	10.52	···	8.64
P_4	4.20	3.90	3.06
P_3	8.94	···	7.25

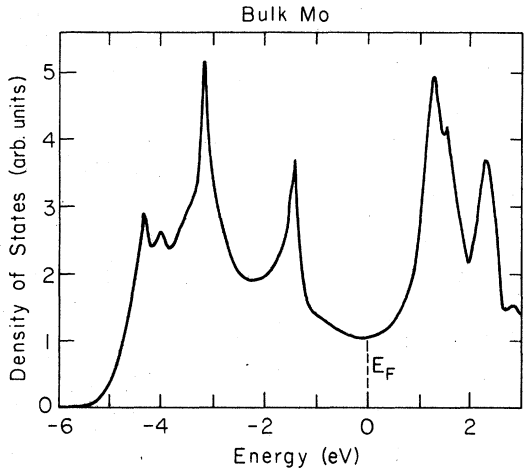

FIG. 3. Density-of-states curve for bulk Mo.

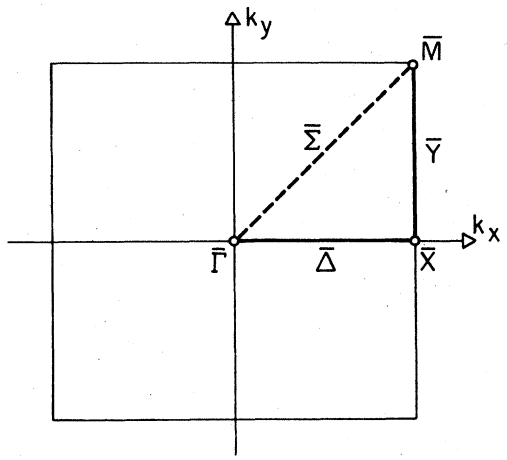

FIG. 4. Surface BZ for Mo(001). The indicated symmetry lines enclose the irreducible part of the zone.

lack of the neighboring atoms.

From the self-consistent potential we recalculated the total valence charge density, the energy levels $E_n(\vec{k}_{\parallel})$, and the electronic wave functions $\psi_n(\vec{k}_{\parallel}, \vec{r})$ at the 15 points, including the symmetry points $\bar{\Gamma}$, $\bar{M}$, and $\bar{X}$ and the symmetry lines $\bar{\Delta}$, $\bar{\Sigma}$, and $\bar{Y}$. $\vec{k}_{\parallel}$ is the wave vector parallel to the surface. This information was used to obtain the local density of states (LDOS) in the various slab regions Ω_i from

$$N_i(E) = \sum_{\vec{k}_{\parallel}, n} \int_{\Omega_i} |\psi_n(\vec{k}_{\parallel}, \vec{r})|^2 \delta(E - E_n(\vec{k}_{\parallel}))\, d^3r \,. \quad (16)$$

To facilitate the analysis of surface states and resonances, we make use of the fact that surface states tend to be localized in $\vec{k}$ space in or near the gaps of the bulk band structure projected onto the surface BZ. We have therefore projected the bulk band structure obtained above onto the symmetry lines $\bar{\Delta}$, $\bar{\Sigma}$, and $\bar{Y}$ and also onto the symmetry points $\bar{\Gamma}$, $\bar{X}$, and $\bar{M}$ using the method described in Ref. 1. The results, together with

TABLE II. Principal peak positions of the bulk density of states obtained from experiment and theory. Energies are given with respect to the Fermi level.

Experiment (photoemission)		Theory		
Ref. 26	Ref. 27	Ref. 21	Ref. 28	This work
−3.6	−3.9	−4.28	−4.0	−4.3
•••	•••	−2.92	3.1	−3.2
−1.6	−1.6	−1.56	1.7	−1.5
•••	1.0	1.50	0.9	1.3
•••	2.0	2.45	1.5	2.3

various calculated surface resonance bands, are shown in Fig. 6(a). The surface states or resonances can be easily characterized by their charge density in real space. In this work we distinguish between a true surface state and a surface resonance by its charge distribution with respect to the surface. A true surface state has its charge confined in the immediate neighborhood of the surface layer with negligible charge inside the slab. In slab calculations these states occur in pairs, with an average energy-level splitting of less than 0.1 eV. A surface resonance has more than 50% of its charge localized at the surface, but the charge can extend quite far into the slab. The resonance also occurs as an energy-level pair, if it is strong enough. The splitting of the levels,

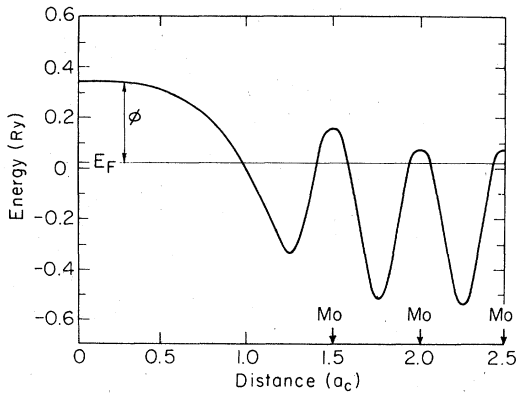

FIG. 5. Self-consistently screened local part of the potential averaged parallel to the (001) surface, plotted as a function of the coordiante z perpendicular to the surface. The positions of the atomic layers are marked by arrows. ϕ is the work function.

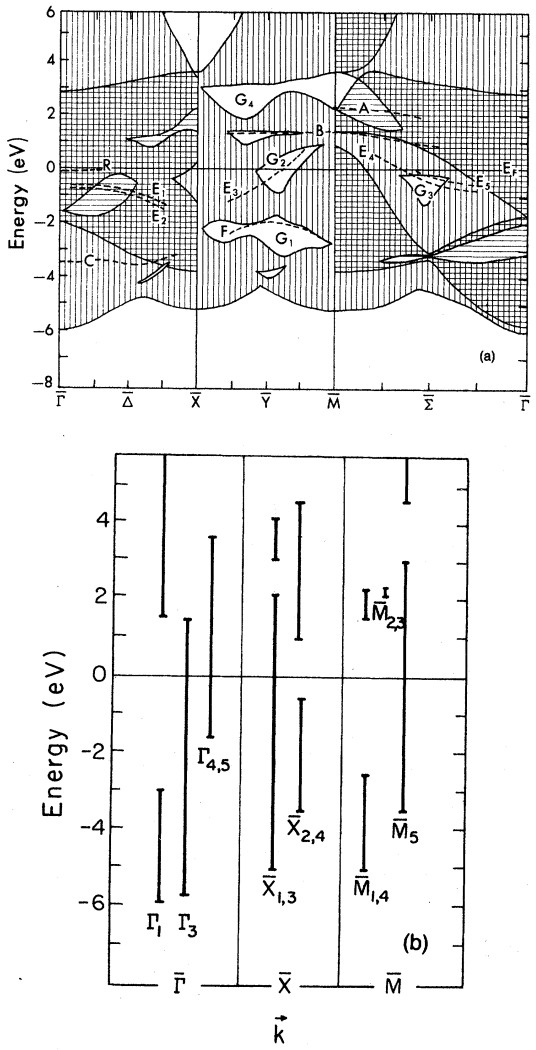

FIG. 6. (a) Projected band structure together with surface resonance bands (dashed lines) along symmetry lines. Vertical cross-hatching is used for states with $\bar{\Delta}_1$, $\bar{Y}_1$, and $\bar{\Sigma}_1$ symmetry and horizontal cross-hatching refers to states with $\bar{\Delta}_2$, $\bar{Y}_2$, and $\bar{\Sigma}_2$ symmetry. (b) Projected band structure for the symmetry points $\bar{\Gamma}$ = (0, 0), $\bar{X}$ = ($\frac{1}{2}$, 0), and $\bar{M}$ = ($\frac{1}{2}$, $\frac{1}{2}$). Character tables for the various irreducible representations are given in Refs. 1 and 28.

however, becomes larger the more the resonance couples to bulk states.

We find a relatively flat resonance band labeled C along $\bar{\Delta}$ around −3.4 eV, which also exists at $\bar{\Gamma}$. The total charge density of this band has $d_{3z^2-r^2}$ and $d_{x^2-y^2}$ character (Fig. 7). The $d_{3z^2-r^2}$ character dominates at $\bar{\Gamma}$, but is overcome by an increasing $d_{x^2-y^2}$ admixture away from $\bar{\Gamma}$. The charge contributions below the surface layer toward the slab interior are relatively small, even though the resonance states are of $\bar{\Delta}_1$ symmetry and can

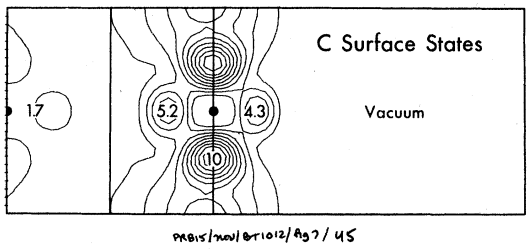

PRB15/nov/BT1012/897/45

FIG. 7. Charge-density contour plot of the C surface states. The contour plane is the (100) plane. Heavy lines represent atomic layers, heavy dots indicate the atomic positions. The charge density is normalized to one electron per unit cell. Successive contours are separated by one-tenth of the maximum density value given in the plot. The first contour away from the maximum therefore has a value of 9.

therefore interact with bulk states of the same symmetry, which exist in this part of the surface BZ. The character of the C resonance state at $\bar{\Gamma}$ is probed by angle-resolved photoemission experiments at normal emission and the whole C band shows up away from normal emission and causes the well-known peak structure at −3.3 eV below E_F.[2-5] Another resonance band F exists in the absolute gap labeled by G_1 along $\bar{Y}$. Its charge has d_{xy} character (Fig. 8). Most of the surface resonance bands are found in an energy interval between E_F and −1.5 eV. Two resonance bands E_1 and E_2 exist in and near the $\bar{\Delta}_1$ symmetry gap along $\bar{\Delta}$. The E_2 band has $d_{3z^2-r^2}$, $d_{x^2-y^2}$, and d_{xz} character; it is therefore of $\bar{\Delta}_1$ symmetry, and consequently shows a much stronger surface localization than the E_1 band, which has d_{zy} and d_{xy} character, and therefore $\bar{\Delta}_2$ symmetry (Fig. 9). Along the $\bar{Y}$ line, we find a resonance band E_3 that can be analytically connected with the band E_4 along $\bar{\Sigma}$ through an absolute gap that extends throughout the irreducible part of the surface BZ connecting the gaps G_2 and G_3 (Fig. 10). E_3 and E_4 have $d_{zx,zy}$ character with an admixture of

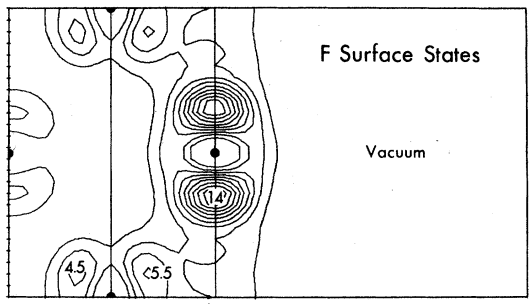

FIG. 8. Charge-density contour plot of the F surface states on the (110) plane. Conventions of Fig. 7.

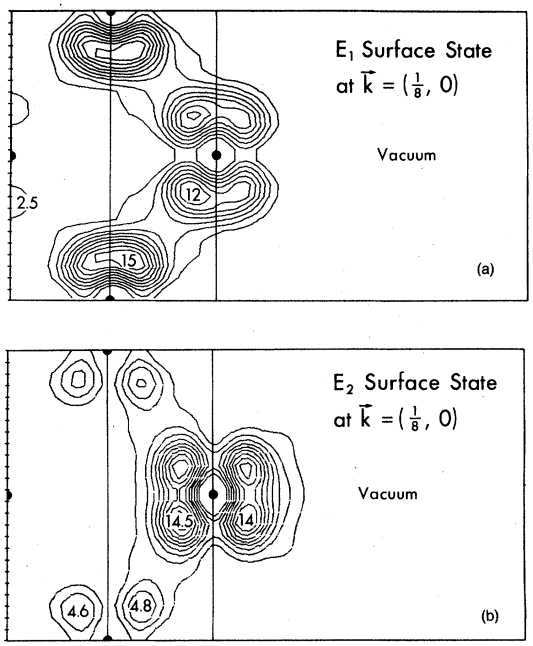

FIG. 9. Charge-density distribution of (a) an E_1 surface state and (b) an E_2 surface state at $\vec{k}=(\frac{1}{8},0)(2\pi/a_c)$ on a (110) plane. Conventions of Fig. 7.

$d_{x^2-y^2}$ (Fig. 11). The resonance band E_5 also has $d_{zx,zy}$ character, but with a d_{xy} mixture (Fig. 12). All the E type states can be derived in a simple orbital picture from the bonding orbitals d_{zx} and d_{zy}, which are broken when the surface is formed. In addition to these dangling-bond-like states, we find a strong surface resonance R around $\bar{\Gamma}$ at -0.2 eV, which becomes a true surface state at $\bar{\Gamma}$ of $d_{3z^2-r^2}$ character (Fig. 13). It exists in a $\bar{\Gamma}_1$ symmetry gap [Fig. 6(b)] and is probed by angle-resolved photoemission at normal emission, giving rise to the sharp peak structure just below the Fermi level.[5] It can also be traced along $\bar{\Sigma}$ as a

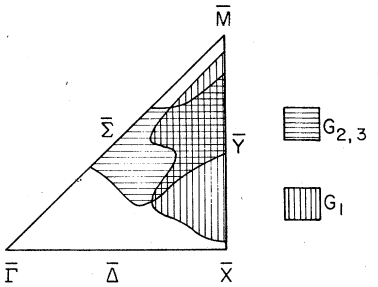

FIG. 10. Extent of the absolute gaps G_1 and G_2 within the irreducible part of the surface BZ. Note the G_2 gap along $\bar{\Sigma}$ is denoted by G_3 in Fig. 6(a).

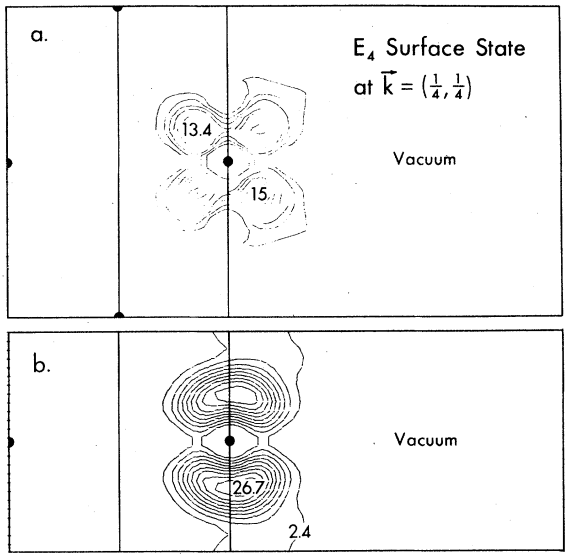

FIG. 11. Charge-density distribution of an E_4 surface state at $\vec{k}=(\frac{1}{4},\frac{1}{4})(2\pi/a_c)$ on (a) a (110) plane and (b) a (100) plane. Conventions of Fig. 7.

relatively weak resonance of $\bar{\Sigma}_1$ symmetry [not shown in Fig. 6(a)]. This state is the result of self-consistency, since it is not present in non-self-consistent calculations. The existence of this state does not depend on contraction of the first interlayer spacing as was proposed in Refs. 4 and 6. In the bond picture, the state can be thought of as being formed by orbitals that split

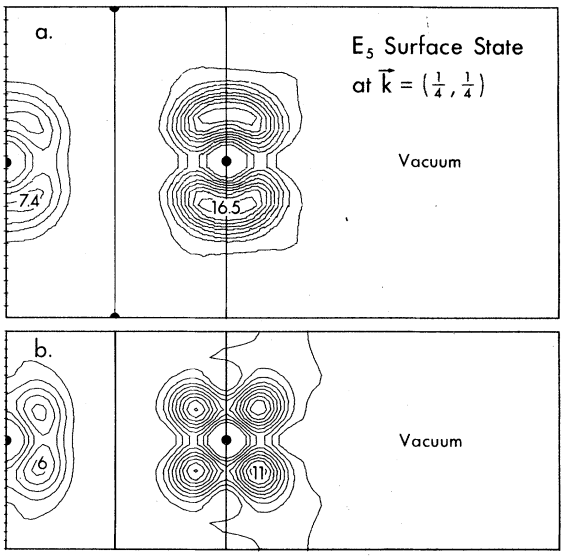

FIG. 12. Charge-density distribution of an E_5 surface state at $\vec{k}=(\frac{1}{4},\frac{1}{4})(2\pi/a_c)$ on (a) a (110) plane and (b) a (100) plane. Conventions of Fig. 7.

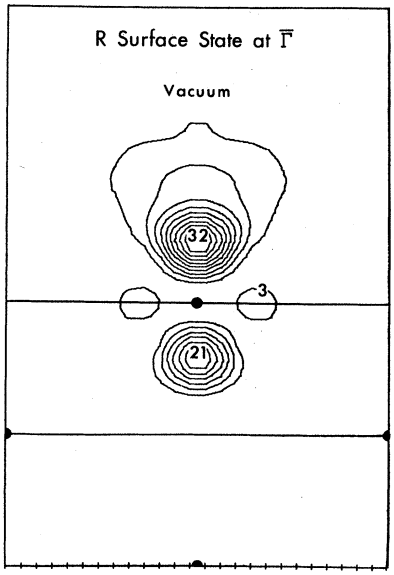

FIG. 13. Charge-density contour plot of a R surface state at $\bar{\Gamma}$ on a (110) plane. Conventions of Fig. 7.

off from the nonbonding part of the $\bar{\Delta}_1$-type bulk states and moves down into the $\bar{\Gamma}_1$ gap so far that it becomes occupied.

Above the Fermi level we find a surface resonance band of distinct $d_{3z^2-r^2}$ character labeled B. It exists mainly in a small absolute gap along $\bar{Y}$ and decays as a resonance along $\bar{\Sigma}$. There is practically no overlap of charge of the B states, which is consistent with the weak dispersion of the B band (Fig. 14). Finally, a true surface state labeled A exists at $\bar{M}$ in the absolute gap G_4 at 2.3 eV. It is solely of $d_{x^2-y^2}$ character and decays rapidly away from $\bar{M}$. The bands A and B also exist in Nb(001). No true surface states are found at $\bar{M}$ in contrast to Nb(001).[1] Since our results for the wave functions and the energy levels are converged within less than 0.2 eV, only the change in

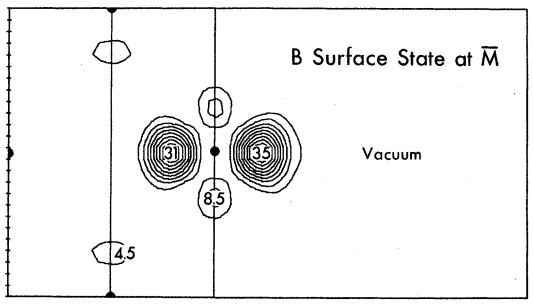

FIG. 14. Charge-density contour plot of a B surface state at $\bar{M}$ on a (110) plane. Conventions of Fig. 7.

the bulk band structure at the N symmetry point can be made responsible for the lack of surface states at $\bar{M}$. With the $N_{1'}$ level higher than the N_1 level the gaps G_2 and G_3 are no longer connected. The gap at $\bar{M}$ that exists in Nb(001) around 3 eV above the Fermi level[1] disappears. The twofold-degenerate surface state of $\bar{M}_5$ symmetry can now couple to bulk states of the same symmetry [Fig. 6(b)], and becomes a very weak resonance in Mo. This result clearly indicates that the rigid-band model does not necessarily hold for predicting surface states.

To compare our results with experiments that are of spectroscopic nature, we have calculated the LDOS at the surface. The result is plotted in Fig. 15. The surface LDOS shows much more structure than the bulk density of states; however, this is partly due to the smaller number of $\vec{k}$ points used, and also to slab effects. To extract surface features we have subtracted the LDOS at the innermost layer from the surface LDOS, keeping only the positive contributions, which represent an excess in electrons at the surface layer as compared to the slab center (shaded areas in Fig. 15). The agreement between our calculated results and experiment is excellent. Besides a low-lying surface resonance structure at −3.3 eV, we find a double-peak structure near the Fermi energy at −0.2 and −0.6 eV. Surface resonances at these energies were found from recent angle-resolved photoemission spectra.[5] In addition, we obtain surface contributions around −2 eV and unoccupied surface resonances, which presumably have not yet been resolved experimentally. All

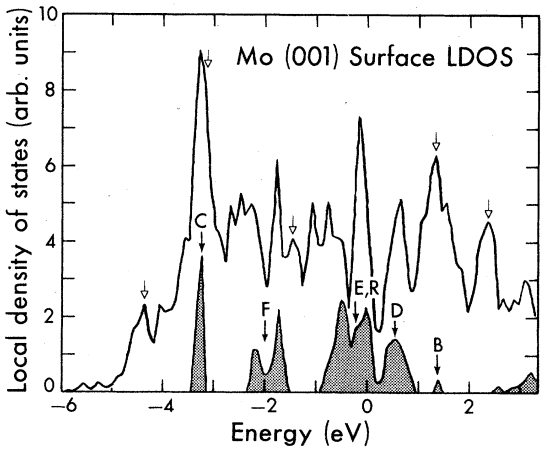

FIG. 15. The local density of states for the surface layer. The shaded areas represent the excess density of states (see text). Energies are measured with respect to the Fermi level. The labeling of the surface states is according to Fig. 6(a). The positions of the principal bulk peaks are marked by open arrows.

surface contributions in the surface LDOS can be uniquely associated with the resonance bands obtained in the $\vec{k}$-space analysis of Fig. 6.

IV. SUMMARY AND CONCLUSION

We have calculated the electric structure of the Mo (001) surface using a self-consistent pseudopotential method that allows for screening of the ionic cores near the surface. The core potentials, which are input to our method, reproduce the bulk properties of Mo in reasonable agreement with other calculations and experiment. A combined set of plane waves and Bloch functions made of localized Gaussian orbitals is employed as basis functions, leading to a very efficient representation of both the highly localized d part and the plane-wave-like s, p part of the cyrstal wave function.

We have analyzed the prominent surface states and resonances in terms of their $\vec{k}$-space behavior in the two-dimensional BZ and in terms of the local density of states. We have also examined the charge-density distribution of the various surface states. Excellent agreement with recent photoemission spectra is obtained. To our knowledge, this is the first self-consistent calculation that reproduces all experimental data satisfactorily. Neither relativistic effects nor surface relaxation is needed to obtain the characteristic structure of this transition-metal surface. Our calculation provides a striking example of the importance of self-consistency at a transition-metal surface. The surface state that exists at the Fermi level at normal emission is not present in non-self-consistent calculations. Noguera *et al.*[4] obtained this state by simulating the self-consistent solution, but a rather large inward contraction of the surface layer was necessary to place the state at the observed energy. Finally, we note that the rigid-band model is only of limited value in predicting surface states. Comparing our results with the results of a similar calculation for the Nb (001) surface, we find that some of the Nb (001) surface states no longer exist at Mo(001), whereas others only occur at Mo(001). Photoemission experiments, however, indicate that surface states at W(001) are most likely to be similar to Mo, both in their extent in $\vec{k}$ space and in their charge-density distribution.

ACKNOWLEDGMENTS

We are grateful to Dr. A. Zunger and Dr. S. G. Louie for helpful discussions on the use of the mixed-basis scheme. This work was supported in part by the Division of Basic Energy Sciences, U. S. Dept. of Energy, and by NSF Grant No. DMR 76-20647-A01. One of us (G.P.K.) was supported by a Deutsche Forschüngsgemeinschaft fellowship.

APPENDIX

The use of a mixed-basis set to represent the crystal wave function requires the calculation of both the Hamiltonian matrix elements $H_{\alpha\alpha'}$ and the overlap matrix elements $S_{\alpha\alpha'}$ in order to diagonalize the eigenvalue problem of Eq. (13). Here, $\alpha\alpha'$ refers to either a plane-wave state $|\vec{k}+\vec{G}\rangle$ or a Bloch state made of localized orbitals $|\Phi_{j\lambda}(\vec{k})\rangle$. To avoid summations over lattice sites and the evaluation of multicenter integrals, we have computed the above matrix elements in reciprocal space whenever it was possible and convenient. For this purpose, we expand the localized-orbital Bloch function in plane waves,

$$\phi_{j\lambda}(\vec{k},\vec{r}) = \frac{1}{\sqrt{NM\Omega_a}} \sum_{\vec{G}} \xi_{j\lambda}(\vec{k},\vec{G})\, e^{i(\vec{k}+\vec{G})\cdot\vec{r}}, \quad \text{(A1)}$$

where the coefficients $\xi_{j\lambda}(\vec{k},\vec{G})$ are given by

$$\xi_{j\lambda}(\vec{k},\vec{G}) = \left(\frac{1}{M}\sum_{\nu} e^{-i\vec{G}\cdot\vec{\tau}_\nu}\theta_{j\nu}\right) \times \left(\frac{1}{\Omega_a}\int e^{-i(\vec{k}+\vec{G})\cdot\vec{r}} d_\lambda(\vec{r})\, d^3r\right). \quad \text{(A2)}$$

N is the number of unit cells, Ω_a is the atomic volume, and M is the number of atoms in a unit cell. Once the expansion coefficients are known, all matrix elements can be calculated in a pure plane-wave representation. We omit the details of this calculation, since they are discussed at length in Ref. 25.

In the case of Mo, the evaluation of the matrix elements $\langle\Phi_{j\lambda}(\vec{k})|\Delta V_{\rm NL}|\Phi_{j'\lambda'}(\vec{k})\rangle$ is facilitated by taking into account that both the d orbitals and the nonlocal d correction to the core potential are extremely short ranged. We can therefore make the so-called on-site approximation

$$\langle\phi_{j'\lambda'}(\vec{k})|\Delta V_{\rm NL}|\phi_{j\lambda}(\vec{k})\rangle \simeq \delta_{jj'}\frac{1}{M\Omega_a}\int d_{\lambda'}(\vec{r}')\Delta v_{\rm NL}(\vec{r},\vec{r}') \times d_\lambda(\vec{r})\, d^3r\, d^3r', \quad \text{(A3)}$$

which contains only a one-center integral. The quality of this approximation can be easily checked by evaluating the exact expression using the plane-wave expansion (A1) of the orbital Bloch functions. The result is practically the same as the result obtained by the on-site approximation.

*Permanent address: Max-Planck-Institut für Festkörperforschung, Büsnauer Strasse 171, D-7000 Stuttgart 80, Federal Republic of Germany.

[1]S. G. Louie, K. M. Ho, J. R. Chelikowsky, and M. L. Cohen, Phys. Rev. B 15, 5627 (1977) and references therein.

[2]R. C. Cinti, E. Al Khoury, B. K. Chakraverty, and N. E. Christensen, Phys. Rev. B 14, 3296 (1976).

[3]Shang-Lin Weng and E. W. Plummer, Solid State Commun. 23, 515 (1977).

[4]C. Noguera, D. Spanjaard, D. Jepsen, Y. Ballu, C. Guillot, J. Lecante, J. Paigne, Y. Petroff, R. Pinchaux, P. Thiry, and R. Cinti, Phys. Rev. Lett. 38, 1171 (1977).

[5]Shang-Lin Weng, T. Gustafsson, and E. W. Plummer, Phys. Rev. Lett. 39, 822 (1977).

[6]C. Noguera, D. Spanjaard, and D. W. Jepsen, Phys. Rev. B 17, 607 (1978).

[7]F. Jona, A. Ignatiev, D. W. Jepsen, and P. M. Marcus, Bull. Am. Phys. Soc. 19, 333 (1974).

[8]E. W. Plummer (private communication).

[9]Shang-Lin Weng, Phys. Rev. Lett. 38, 434 (1977).

[10]G. P. Kerker, K. M. Ho, and M. L. Cohen, Phys. Rev. Lett. 40, 1593 (1978).

[11]J. C. Slater, Phys. Rev. 81, 385 (1951).

[12]W. Kohn and L. J. Sham, Phys. Rev. 170, 1133 (1965).

[13]F. Herman and S. Skillman, *Atomic Structure Calculations* (Prentice-Hall, Englewood Cliffs, 1963).

[14]A similar approach was used by R. N. Euwema, Phys. Rev. B 4, 4332 (1971) for bulk Nb.

[15]S. L. Altmann and A. P. Cracknell, Rev. Mod. Phys. 37, 19 (1965).

[16]See, for example, R. N. Euwema, D. J. Stukel, and T. C. Collins, in *Computational Methods in Band Theory*, edited by P. M. Marcus, J. F. Janak, and A. R. Williams (Plenum, New York, 1971).

[17]P. O. Löwdin, in *Proceedings of the Internat. Symposium No. 1 on Atomic, Molecular, and Solid State Theory*, 1967, edited by P. O. Löwdin (Interscience, Wiley, New York, 1967), p. 811.

[18]See, for example, M. Schlüter, J. R. Chelikowsky, S. G. Louie, and M. L. Cohen, Phys. Rev. B 12, 4200 (1975).

[19]S. G. Louie, K. M. Ho, and M. L. Cohen (unpublished).

[20]D. J. Chadi and M. L. Cohen, Phys. Rev. B 8, 5747 (1973).

[21]I. Petroff and C. R. Viswanathan, Phys. Rev. B 4, 799 (1971).

[22]V. L. Moruzzi, J. F. Janak, and A. R. Williams (unpublished). We thank these authors for supplying information on their results.

[23]J. W. Cooley and J. W. Tukey, Mat. Comp. 19, 297 (1965); A. Zunger, G. P. Kerker, and M. L. Cohen (unpublished).

[24]S. L. Cunningham, Phys. Rev. B 10, 4988 (1974).

[25]J. R. Chelikowsky and M. L. Cohen, Phys. Rev. B 14, 556 (1976).

[26]D. E. Eastman, Solid State Commun. 7, 1697 (1969).

[27]K. A. Kress and G.J. Lapeyre, in *Electronic Density of States, Third Materials Research Symposium, Gaithersburg, Md., 1969*, edited by L. H. Bennett, Natl. Bur. Stds. Publ. No. 323 (U.S. GPO, Washington, D.C., 1971), p. 209.

[28]L. M. Falicov, in *Group Theory and Its Physical Applications* (University of Chicago, Chicago, 1966).